GEOPHYSICAL RESEARCH LETTERS, VOL. 24, NO. 5, PAGES 555-558, MARCH 1, 1997

Observations of the annual cycle of sea ice temperature and mass balance

Donald K. Perovich, Bruce C. Elder, and Jacqueline A. Richter-Menge

U.S. Army Cold Regions Research and Engineering Laboratory, 72 Lyme Road, Hanover, NH

Abstract. A vertical array of thermistors coupled with an autonomous data-logging system was used to obtain a 15-month record of ice temperature profiles in a multiyear floe in the Beaufort Sea. This record was used to monitor atmosphere, ice and ocean temperatures, determine changes in the ice mass balance, and infer estimates of the ocean heat flux and the snow thermal conductivity. Ablation during the summer melt season consisted of approximately 0.3 m of snow melt, 0.67 m of ice surface ablation and 0.25 m of bottom ablation. There was 0.45 m of bottom accretion during the growth season. The annually averaged ocean heat flux was 4 W m^{-2}, with a summertime value of 9 W m^{-2}. Comparing these results to earlier studies conducted in the same region showed considerable interannual variability in summer melting. The thermal conductivity of snow cover was approximately 0.3 W m^{-1} K^{-1} during winter.

Introduction

The Arctic sea ice cover plays a major role in governing the exchange of energy between the ocean and atmosphere in the polar regions. Results of global climate change models indicate that there is still much to be learned about the details of the complex atmosphere–ice–ocean interaction (Rind et al., 1995). The key to improving this understanding is the collection of field measurements pertinent to the development of physically based parameterizations of sea ice thermodynamic processes. A basic element in studies focused on thermodynamics is the mass balance of the ice cover (Hanson, 1965; Koerner, 1973). Coupled with ice temperature measurements, mass balance measurements provide valuable information on the heat exchange among the air, ice and ocean (Untersteiner, 1961; McPhee and Untersteiner, 1982; Wettlaufer, 1991).

Making direct measurements of the mass balance is straightforward. Typically an array of stakes and thickness gauges is used to measure ablation and accumulation of ice and snow at the top and bottom of the ice cover (Untersteiner, 1961; Hanson, 1965; Koerner, 1973). The mass balance of sea ice can also be inferred from temperature profile measurements (Perovich et al. 1989).

In spite of the importance of mass balance measurements and the relatively simple equipment involved in making them, there are few observational results. This is due, in large part, to the expense involved in operating a long-term field camp, which typically serves as the base for these studies. The combined results of four sea ice mass balance studies (Untersteiner, 1961; Hanson, 1965; Koerner, 1973; Maykut and McPhee, 1995) suggest that there is significant interannual variability in the ablation/accretion rate of the sea ice cover. Measurements of the total ablation of unponded, level multiyear ice over the summer season range from 39 to 60 cm. As discussed in Untersteiner (1961) and Hanson (1965), the interannual variability at a particular latitude may be greater than variability at different latitudes in a single year.

In this paper we present a 15-month temperature record of the atmosphere, ice and ocean which was collected autonomously. The measurement site was installed at the center of a multiyear floe in the Alaskan Beaufort Sea and, as such, represents a single point measurement. This approach is not appropriate for gaining a detailed understanding of the temporal variations in heat and mass balance due to the influence of the variable top and bottom surface topography, typical of multiyear floes (Wettlaufer, 1991). As McPhee and Untersteiner (1982) point out, however, it does lend itself to studies that consider long time periods, since overall changes in the ice temperature profile are bound to be large compared to the errors of a single measurement. With this in mind, the record will be used to examine the temperature evolution of the ice as it progresses through a complete annual cycle. The temperature profiles will also be used to infer the snow and ice mass balance and estimate the oceanic heat flux and thermal conductivity of the snow on a seasonal basis. These results will be compared to field and theoretical studies.

Data Acquisition

In late September 1993 an ice camp was established in the Alaskan Beaufort Sea to support the six-month, Office of Naval Research-sponsored Sea Ice Mechanics (SIMI) field program. The temperature measurement site was located near the center of a 2-km-diameter multiyear floe that served as a base for the SIMI ice camp. The temperature profile in the ice, and the adjacent atmosphere and ocean, was obtained using a string of 48 thermistors, mounted on solid 3.2-cm-diameter PVC rods that were frozen into the ice. At the time of installation, the ice was 2.13 m thick, with no snow on the surface. Thermistors extended 55 cm above and 345 cm below the ice surface, at a spacing of 5, 10 or 20 cm. The closest spacing was at the ice/air interface and in the water column near the bottom of the ice. To minimize the effects of solar radiation, the thermistor string was painted white. The accuracy of the thermistors is ±0.1°C. Temperatures were measured and recorded hourly using a Campbell Scientific CR10 datalogging and storage system.

Using this setup we were able to measure and store temperature profiles from October 1993 until December 1994, eight months beyond the end of the SIMI field experiment. The periods when there were personnel at the site allowed for manual measurements of the snow cover and ice thickness at the data collection site and other locations on the multiyear floe. The equipment at the data collection site was recovered during a final visit to the floe on 29

Paper number 97GL00185.

April 1995, when one last set of measurements was taken to define the state of the ice and snow cover after the second winter had passed.

Results and Discussion

Temperature

The 15-month-long record of air, ice and ocean temperature is summarized in Figure 1. The air temperature was measured using the top thermistor, which was between 20 and 120 cm above the surface, depending on the snow depth and the amount of surface ablation. The annual cycle of air temperature is evident in Figure 1a. During the summer, air temperatures were fairly constant near 0°C, and there was a gradual decrease in the fall and increase in the spring. In the winter there was considerable variation in air temperature, with minimum temperatures of approximately –40°C. There was a major warming event on 25 January when air temperatures increased by more than 30°C to values near 0°C. During fall and winter, changes of more than 10°C in a day or two were common. These warming events occurred at roughly 6- to 8-day intervals, consistent with the observed periodicity of synoptic-scale weather systems in the Beaufort Sea area. The first sunrise at the floe occurred in early February, and by the beginning of March there were 10 hours of sunlight daily. At this time a distinct diurnal cycle in air temperature became evident. This diurnal signal was strong throughout the spring, was present to a lesser extent in the summer, and had faded away by the end of September.

Contours of ice temperature are plotted in Figure 1b. Seasonal trends in ice temperature are consistent with previous observations (Untersteiner, 1961) and model results (Maykut and Untersteiner, 1971). In late summer the ice began to cool, and throughout the fall this cooling propagated down through the ice, reaching the bottom in mid-December. At this point the ice sheet began to thicken by bottom accretion. During the winter the ice cooling and bottom accretion continued. There was significant

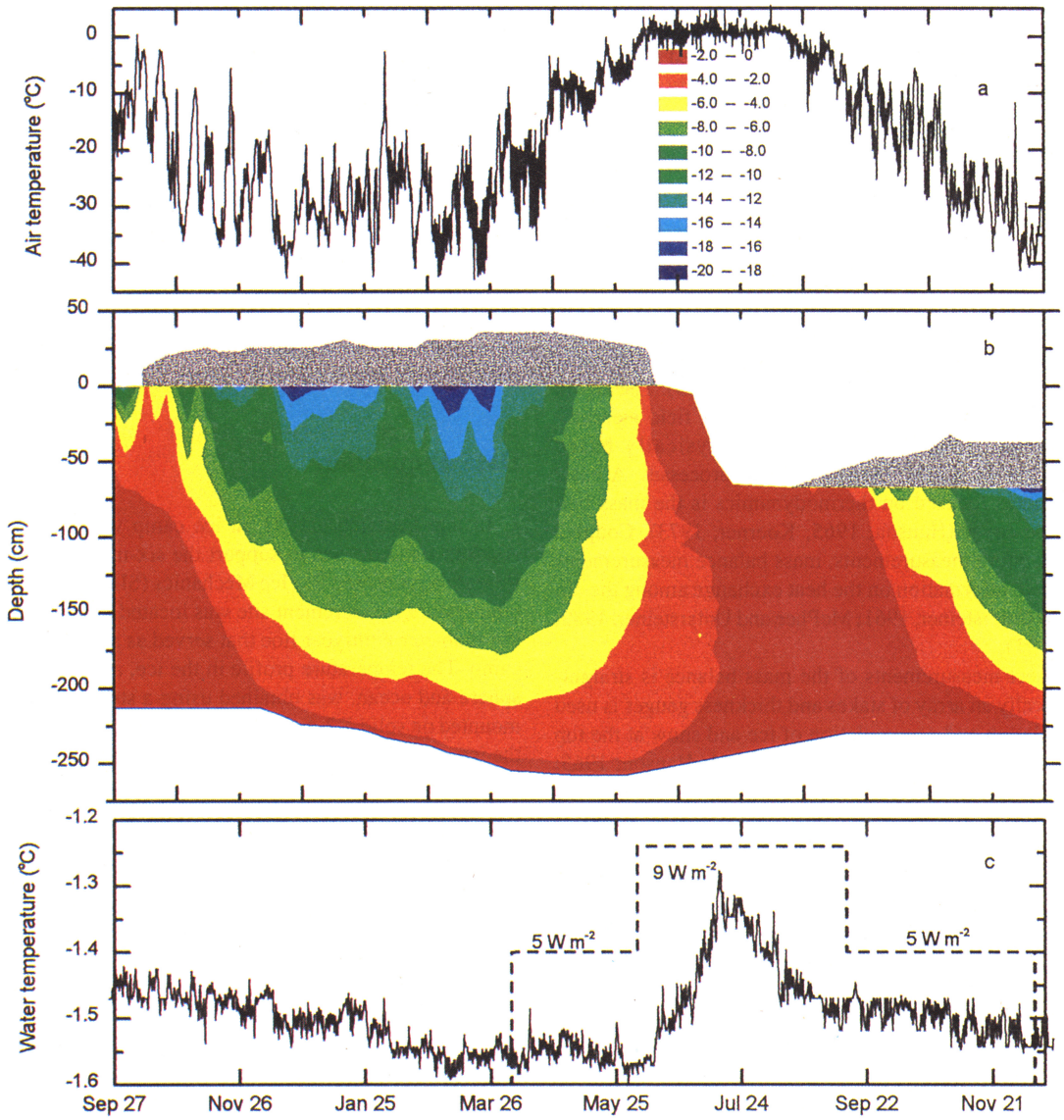

Figure 1. Time series of a) air temperature, b) internal ice temperature and c) upper ocean temperature from 27 September 1993 to 16 December 1994. The gray shaded area in b) denotes the snow cover; the temperature contours are bounded by the surface and bottom of the ice.

warming of the upper portion of the ice in late January in response to near –0°C air temperature. As the air temperature increased in the spring, the ice began to warm. Surface melting began in early June, and by early July the ice temperature was nearly isothermal at –1°C ±0.5°C. By mid-August the melt season had ended and fall freeze-up had begun.

Water temperatures near the bottom of the ice are plotted in Figure 1c. These temperatures were measured 320 cm from the surface of the ice, which was approximately 60 cm beneath the ice in June of 1994. For the most part, temperatures were between –1.45°C and –1.6°C. A slight warming of the water was noticeable in June, and this warming became more distinct during the summer, reaching temperatures as high as –1.25°C. Temperatures decreased in September returning to values near –1.5°C. No observations of the upper ocean salinity were made during summer when the camp was unmanned. Thus, it is not clear if the water was still at its salinity-determined freezing point and the temperature increase was in response to a freshening of the upper ocean or if the water warmed above freezing.

Mass balance

For much of the year, the temperature profiles from our thermistor string can be used to infer the position of the snow surface, ice surface and ice bottom to within ±1–2 cm. Air/snow, snow/ice and ice/water interfaces are denoted by discontinuities in the temperature profile. A sequence of temperature profiles can be used to monitor the temporal changes in the position of these interfaces, and therefore the mass balance of the ice. This method is severely limited during the summer melt season when there is no significant thermal contrast between the lower portion of the ice and the upper part of the water column. The position of the ice surface can still be estimated since air temperatures are typically slightly above 0°C.

The time history of snow accumulation and ablation and ice accretion and ablation is plotted in Figure 1b. At installation on 27 September the ice was 213 cm thick and there was no snow present. Snow depth increased rapidly in early fall to approximately 25 cm, then continued to increase slowly throughout the winter to a maximum value of 35 cm. Throughout this period there were fluctuations in snow depth of roughly ±5 cm due to wind transport of snow. The snow cover melted rapidly in one week from 8 June to 14 June, and the surface remained free of any appreciable amount of snow until the end of August. With the snow cover gone, ice surface ablation began. Ablation was slow the first two weeks, became more rapid in July, and finally tapered off in early August. By 20 August there was new snow on the surface and fall freeze-up had begun. The total ablation on the surface during the summer melt season was 30 cm of snowmelt and 67 cm of ice ablation. Snow accumulation between August 1994 and December 1994 totaled 30 cm, with most of the snowfall occurring in September and October. The rapid cooling observed during fall freeze-up above a depth of 67 cm indicated that, at least at the end of summer, the thermistor string was not in a melt pond.

There was little change in mass at the underside of the ice during the autumn of 1993. Beginning in mid-December there was steady ice growth until April, when the growth rate slowed appreciably. Growth ended and ablation began in early June. The ice thickness increased from 213 cm in September 1993 to 258 cm in June 1994, then decreased to approximately 166 cm in September 1994. Thus there was 45 cm of bottom accretion during the growth season and 25 cm of bottom ablation during the melt season. This indicates that the total heat input to the ice cover during the primary melt period from 4 June to 12 September was 361 MJ m^{-2}. Surface melting accounted for 55% of the heat input, while bottom ablation was 22%, ice warming was 14%, and snowmelt was 9%. The total heat input during this period was equivalent to an average net flux into the ice cover of 42 W m^{-2}.

Results have been reported from other mass balance studies conducted in this same general region during ice station Alpha II in 1959 (Hanson, 1965) and during AIDJEX in 1975 (Maykut and McPhee, 1995). Surface melting during Alpha II began on 20 June and ended 12 August, and there was a total of 38 cm of surface ablation on unponded ice and 11 cm of bottom ablation (Hanson, 1965). Surface ablation in ponded ice was notably greater, totaling 85 cm. During AIDJEX the average ablation for unponded ice was 26 cm on the surface and 34 cm on the bottom (Maykut and McPhee, 1995). Total ablation during SIMI was 50% greater than observed during AIDJEX and nearly double that observed during Alpha II on unponded ice. In both SIMI and Alpha II, surface ablation was two to three times larger than bottom ablation, consistent with observations made at more northerly latitudes (Untersteiner, 1961; Hanson, 1965; Koerner, 1973). This is in contrast to the AIDJEX data, where bottom ablation was greater. Comparing results from these three cases illustrates the considerable interannual variability present in summer ice ablation. This is in keeping with the earlier finding (Untersteiner, 1961; Hanson, 1965) that interannual variability at a particular latitude can be greater than variability at different latitudes in a single year.

A key issue is what causes this variability in ablation. There are several possible factors, including the snow depth in late spring, the occurrence of the first snowfall in early autumn, the surface albedo, the pond fraction during the melt season, the amount of open water present and the cloudiness (Jin et al., 1994; Ebert et al., 1995). At present the importance of these factors, and the sensitivity of the mass balance to small perturbations in them, is not known.

Ocean heat flux

Ice temperature profiles, combined with measurements of bottom ablation and accretion, have been used to estimate the time-averaged ocean heat flux (F_w) (McPhee and Untersteiner, 1982; Perovich et al., 1989; Wettlaufer, 1991). In this method the time-averaged ocean heat flux is calculated as a residual of the conductive, specific and latent heat: $F_w = 1/\Delta t\ (Q_f + Q_s + Q_l)$. A reference depth, in this case 175 cm, is selected in the ice. The heat conducted through this level (Q_f), the cooling or warming of the ice below the level (Q_s) and the latent heat of freezing or melting (Q_l) are all calculated as a function of time. The Q's are computed using standard relationships for the conductive, specific and latent heats (Wettlaufer, 1991), with the ice salinity and density and the time series of temperature and changes in mass at the ice bottom used as input parameters. In our measurements the largest uncertainty is in the amount of bottom ablation or accretion, and thus Q_l. Except for the summer, we can estimate mass changes at the ice bottom to within ±2 cm. To minimize the effects of this uncertainty, we have averaged over time intervals of at least 60 days, giving an uncertainty in Q_l of 3–6 MJ m^{-2} and F_w of 1–2 W m^{-2}. Another limitation of this analysis is that it is a single-point measurement of ocean heat flux. Wettlaufer (1991), in a study conducted in the eastern Arctic northeast of Fram Strait, showed large variations measured at different sites on a single floe due to small-scale topography of the underside of the ice and instabilities in the ice/ocean boundary layer. Measurements made in the Beaufort Sea during AIDJEX at four sites in multiyear ice showed little spatial

variability in bottom ablation rates during June and July, but significant differences of 0.5 cm day^{-1} in August (Maykut and McPhee, 1996). Morphological studies on the SIMI floe indicated that the temperature site was situated in relatively undeformed area of multiyear ice, where under-ice topographic influences were small.

The annual average of the ocean heat flux was 4 W m^{-2}, comparable to the value of 3.5 W m^{-2} determined from mass balance data by Maykut and McPhee (1995) for AIDJEX. The four subperiods, representing the period of rapid growth during winter, slow growth during spring, ablation during summer and the gradual cooling of the ice in fall, illustrate the strong seasonal dependence of the ocean heat flux. During winter, F_w was essentially zero. In the spring, F_w increased to 5 W m^{-2} as the incident solar radiation and the heat input to the water column increased. The maximum average value of F_w = 9 W m^{-2} was observed during the summer melt when the heat input to the water column was a maximum. Based on the results of Maykut and McPhee (1995), we expect that there were peak values of F_w during the summer that were considerably higher than this average, but without a direct means of measuring bottom ablation during summer we can only compute values averaged over the entire summer. The fall average of 5 W m^{-2} probably results from the extraction of the remainder of the solar heat deposited in the upper ocean during the summer. Maykut and McPhee (1995) reported values of F_w determined from direct ocean turbulent heat flux measurements at four sites during AIDJEX. F_w time-averaged from late May through October ranged from 10 to 14 W m^{-2}, 25% to 75% higher than the 9 W m^{-2} measured for the same time of year during this experiment.

Snow conductivity

The thermal insulating properties of a snow cover, and its impact on ice growth, are well established. Because of this, knowing the thermal conductivity of snow is important for sea ice thermodynamic modeling studies. Numerous observations in the Arctic and at lower latitudes have determined that the thermal conductivity of snow varies over a wide range of values (Sturm et al., 1997), creating some uncertainty as to the appropriate value to use for the snow cover on sea ice. At the SIMI site the snow cover was typical of that found on multiyear Arctic sea ice. It was primarily a wind-packed slab with a density between 0.30 and 0.35 g cm^{-3} and a thin layer of depth hoar at the base. The temperature record can be used to estimate *in situ* the thermal conductivity of the snow cover on sea ice. To do this, we exploit the continuity of heat flux at the snow/ice interface, $k_s(dT_s/dz) = k_i(dT_i/dz)$, where T_s is snow temperature, T_i is ice temperature and z is the vertical position within the snow or ice. The upper portion of the ice cover was desalinated so its thermal conductivity (k_i) was that of fresh ice, 2.04 W m^{-1} K^{-1}. The temperature data can be used to compute the temperature gradients in the snow and ice and thus to determine k_s. However, accurately determining the gradients is not trivial, as the temperature profiles may be affected by such factors as transient temperature pulses or solar heating (Zhang and Osterkamp, 1995). To simplify the determination of the temperature gradients and to improve the quality of the calculated k_s, we selected periods that satisfied four criteria: air temperatures were stable and cold, there were no significant transients, the temperature gradients were linear, and there was no solar heating of the snow or ice. Using these criteria we determined k_s on 16 November, 16 December and 15 January (Figure 1). Snow depths for these cases were between 30 and 35 cm and snow temperatures ranged from −17° to −33°C. Temperature profiles in the snow and in the upper layer of the ice were each fitted to linear equations and the gradients computed. Calculated conductivities were similar in all three cases, with values of 0.30 W m^{-1} K^{-1} on 16 November, 0.29 W m^{-1} K^{-1} on 16 December and 0.31 W m^{-1} K^{-1} on 15 January. Uncertainties for k_s are ±0.01 W m^{-1} K^{-1}. These results are within the range for hard wind-packed slabs on terrestrial substrates reported by Sturm et al. (1997) and, we feel, are representative of the cold, wind-packed snow that covers Arctic sea ice for much of the year.

Conclusions

Snow depths were approximately 30–35 cm for much of the year, and the snow thermal conductivity during winter was 0.30 W m^{-1} K^{-1}. Over an annual cycle there was 67 cm of surface ablation and 25 cm of bottom ablation during the melt season, with 45 cm of bottom accretion during the growth season. The annually averaged ocean heat flux was 4 W m^{-2}, with a summertime value of 9 W m^{-2}. Comparing these results to earlier observations in the same region demonstrates the considerable interannual variability present in summer ice decay.

Acknowledgments. We thank Jay Ardai for his able assistance in deploying and retrieving the instrumentation. This worked was funded by the Office of Naval research (Contract Number N0001496MP30028) and the National Science Foundation, Office of Polar Programs, Arctic Systems Science (OPP-9504311).

References

Ebert, E. E., J. L. Schramm, and J. A. Curry, Disposition of solar radiation in sea ice and the upper ocean, *J. Geophys. Res., 100*, 15965–15975, 1995.

Grenfell, T. C., and G. A. Maykut, The optical properties of ice and snow in the Arctic Basin, *J. Glaciol., 18*, 445–463, 1977.

Hanson, A. M., Studies of the mass budget of Arctic ice pack floes, *J. Glaciol., 5*, 701–709, 1965.

Jin, Z., K. Stamnes, and W. F. Weeks, The effect of sea ice on the solar energy budget in the atmosphere-sea ice-ocean system: A model study, *J. Geophys. Res., 99* (C12), 25281–25294, 1994.

Koerner, R. M., The mass balance of the sea ice of the Arctic Ocean, *J. Glaciol., 12*, 173–185, 1973.

Maykut, G. A., and M. G. McPhee, Solar heating of the Arctic mixed layer, *J. Geophys. Res., 100*, 24691–24703, 1995.

Maykut, G. A., and N. Untersteiner, Some results from a time dependent, thermodynamic model of sea ice, *J. Geophys. Res., 76*, 1550–1575, 1971.

McPhee, M. G., and N. Untersteiner, Using sea ice to measure vertical heat flux in the ocean, *J. Geophys. Res., 87*, 2071–2074, 1982.

Perovich, D. K., W. B. Tucker III, and R. A. Kirshfield, Oceanic heat flux in Fram Strait measured by a drifting buoy, *Geophys. Res. Let., 16*, 995–998, 1989.

Rind, D., R. Healy, C. Parkinson, and D. Martinson, The role of sea ice in $2 \times CO_2$ climate model sensitivity. Part I: The total influence of sea ice thickness and extent, *J. of Climate*, 450–463, 1995.

Sturm, M., J. Holmgren, M. Konig, and K. Morris, The thermal conductivity of seasonal snow, *J. Glaciol.*, 1997.

Untersteiner, N., On the mass and heat budget of Arctic sea ice, *Arch. Meteorol. Geophys. Bioklim., Ser. A, 12*, 151–182, 1961.

Wettlaufer, J. S., Heat flux at the ice–ocean interface, *J. Geophys. Res., 96*, 7215–7236, 1991.

Zhang, T., and T. E. Osterkamp, Considerations in determining thermal diffusivity from temperature time series using finite difference methods, *Cold Reg. Sci. Tech., 23*, 333–341, 1995.

(Received December 6, 1996; accepted January 6, 1997.)